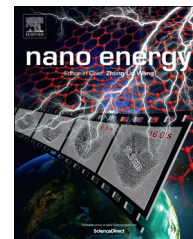




Available online at www.sciencedirect.com

ScienceDirect

journal homepage: www.elsevier.com/locate/nanoenergy



RAPID COMMUNICATION

Tandem structured spectrally selective coating layer of copper oxide nanowires combined with cobalt oxide nanoparticles



Tae Kyoung Kim^{a,c}, Bryan VanSaders^{a,b,c}, Jaeyun Moon^d,
Taewoo Kim^{a,c}, Chin-Hung Liu^{a,c}, Jirapon Khamwannah^{a,c},
Dongwon Chun^{a,c}, Duyoung Choi^{a,c}, Alireza Kargar^{a,c},
Renkun Chen^{a,c}, Zhaowei Liu^b, Sungho Jin^{a,c,*}

^aMaterials Science & Engineering, University of California at San Diego, 9500 Gilman Dr., La Jolla, CA 92093, USA

^bElectrical & Computer Engineering, University of California at San Diego, 9500 Gilman Dr., La Jolla, CA 92093, USA

^cMechanical and Aerospace Engineering, University of California at San Diego, 9500 Gilman Dr., La Jolla, CA 92093, USA

^dMechanical Engineering, University of Nevada at Las Vegas, 4505 S. Maryland Pkwy., Las Vegas, NV 89154, USA

Received 27 August 2014; received in revised form 21 October 2014; accepted 22 October 2014
Available online 28 October 2014

KEYWORDS

Tandem structure;
Spectrally selective coating (SSC) layer;
Copper oxide nanowires;
Cobalt oxide nanoparticles;
Solar absorption;
Solar thermal

Abstract

Increasing the light absorption across the wide solar spectrum has important implications for applications in solar-thermal and photovoltaic energy conversion. Here, we report novel tandem structures combining two different materials with complementary optical properties and microstructures: copper oxide (CuO) nanowires (NWs) and cobalt oxide (Co₃O₄) nanoparticles (NPs). Copper oxide NWs of 100-200 nm in diameter and 5 μm long are grown thermally on copper foil in air and cobalt oxide NPs of 100-200 nm in diameter are synthesized hydrothermally. Tandem structures of spectrally selective coating (SSC) layer are built with three different methods: spray-coating, dip-coating of cobalt oxide NPs into copper oxide NWs forest, and transferring of copper oxide NWs layer onto cobalt oxide NPs layer. The tandem-structured SSC layers fabricated from the spray-coating, dip-coating and transferring methods exhibit figure of merit (FOM) values of 0.875, 0.892 and 0.886, respectively, which are significantly higher than that of the starting copper oxide NWs (FOM=0.858) and cobalt oxide NPs

*Corresponding author at: Materials Science & Engineering, University of California at San Diego, 9500 Gilman Dr., La Jolla, CA 92093, USA.
E-mail address: jin@ucsd.edu (S. Jin).

(FOM=0.853). Our results demonstrate the efficacy of using novel tandem structures for enhanced light absorption of solar spectrum, which will find broad applications in solar energy conversion.

© 2014 Elsevier Ltd. All rights reserved.

Introduction

The Earth receives an enormous amount of incoming solar radiation generated by fusion reaction in the sun, which is expected to remain stable for the next 4 billion years [1,2]. Therefore, solar energy is the most plentiful resource for energy supply. Photovoltaic (PV) solar cells, concentrating solar power (CSP) systems, solar thermoelectric generators as well as photoelectrochemical water splitting systems harvest solar energy for electricity or fuel [3-8].

CSP system uses heliostat mirror arrays to concentrate sunlight to the spectrally selective coating (SSC) layer on the solar receiver structure (such as a corrosion-resistant Inconel alloy tube) to heat up a heat transfer fluid inside (e.g., a molten salt), which is then transported to create high-pressure steam and utilized to drive a steam-turbine-type heat engine to generate electricity. The CSP system is already commercialized with a multi-gigawatt level power generations, with a fast industrial growth in progress, especially with a recent recognition of CSP's advantage of potentially inexpensive energy storage (e.g., by using molten salt reservoir), which can be quite useful and beneficial for control of energy distribution in energy grid systems [4].

Among many approaches to increase the efficiency of solar-based energy conversion devices, nanowire (NW) structures have been used for enhanced light absorption and charge separation, such as demonstrated in Si micro-nanowires for PV solar cells [9-12] and copper oxide NWs for photoelectrochemical water splitting systems [13,14]. For CSP type solar thermal applications, Si NWs are not suitable because the band gap of Si (1.12 eV at 300 K [15]) is not sufficiently low to absorb near-infrared (IR) sunlight spectrum and pure Si can be easily oxidized when exposed to air at high temperature. For instance, ~ 45 nm of silicon oxide will grow on Si when it is annealed at 700 °C for 100 h under dry oxygen atmosphere [16] and Si nanoparticle has been reported to increase its weight by ~ 15 wt% through the oxidation at 750 °C for 2 h in dry oxygen [17]. In this regard, copper oxide (CuO) is a better candidate material because it is already oxidized into a stable oxide form and should be resistant to oxidation in air. For highly efficient CSP system, it is desirable that the SSC layers absorb as much sunlight as possible with high absorption and low sunlight reflectivity in the visible and near-IR spectrum range and have high reflection in the spectrum range longer than near-IR to obtain low thermal emission. The wavelength regime of interest for CSP solar energy absorption includes the visible spectrum range ($< \sim 700$ nm) and near IR spectrum range (~ 700 nm to 1.6 μ m). Based on our measurements, copper oxide NWs exhibit relatively high sunlight reflection characteristics in near-IR spectrum, even though the reflection in visible spectrum is quite low. Copper oxide (CuO) has been reported to have band gap of 1.2-1.4 eV which corresponds to the

absorption from the wavelength of 890-1030 nm [18,19]. This optical property of CuO results in high reflectance of near-IR spectrum longer than 890-1030 nm. Therefore, it is necessary to combine another near-IR absorbing material layer with copper oxide NWs structure, which could then enable efficient sunlight absorption over a broader spectrum range.

As a desirable material to absorb near-IR spectrum, semiconducting metal oxides with small band gap can be utilized. For example, one phase of cobalt oxide, Co_3O_4 , has absorption bands at several spectrum ranges including 0.82-0.85 eV (~ 1500 nm), 0.93-1.03 eV (1340-1200 nm), 1.5-2.07 eV (850-700 nm) and 1.88-3.1 eV (660-400 nm) [20-24] which means Co_3O_4 can become a candidate to increase the absorption of near-IR spectrum when combined with copper oxide NWs structure. We have introduced a hybrid structure containing both Co_3O_4 and Cu oxide NWs so as to broaden

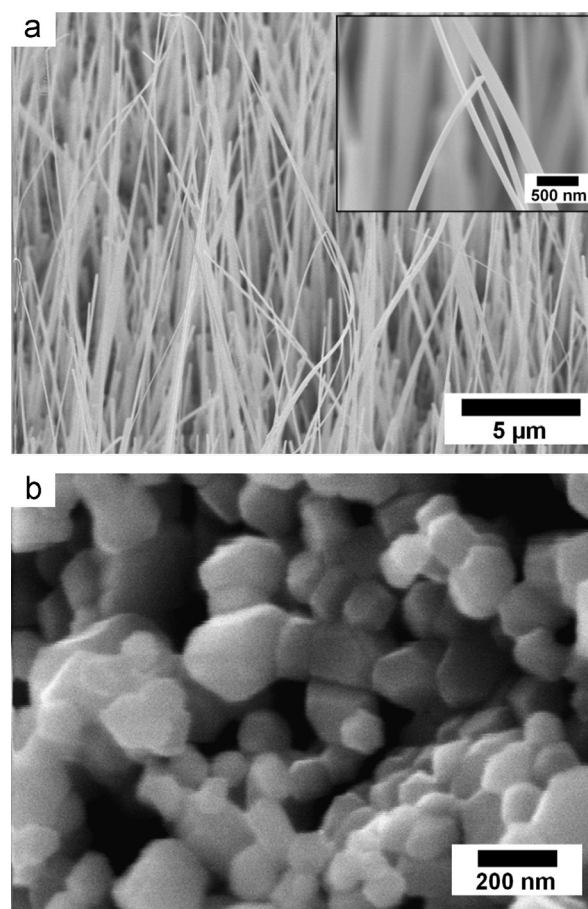


Figure 1 SEM images observed for (a) copper oxide NWs longer than 5 μ m with a diameter of 100-200 nm and (b) cobalt oxide NPs having mainly 100-200 nm in particle size.

the absorbed spectrum range of sunlight. Such a ‘tandem structure’ approach has also been used in PV solar cells to absorb different spectrum ranges using a combination of materials or different sized quantum dots having different band gaps [25–27], however, such an approach has not been investigated much in the case of CSP solar absorber materials.

In this work, new tandem structures of SSC layer having copper oxide NWs and cobalt oxide (Co_3O_4) NPs have been prepared by scalable spray-coating or dip-coating type processes. Our results indicate that this tandem structure of SSC layers significantly increases the absorption of sunlight, which is expected to improve the energy conversion efficiency of solar thermal systems such as CSP and solar thermoelectric generation systems.

Materials and methods

Thermal growth of copper oxide nanowires

Thermal growth of copper oxide nanowires (NWs) was made by annealing copper foil in air atmosphere [13,14]. As a pretreatment procedure, the purchased copper foil (Alfa Aesar, 50 μm thick) was cleaned with hexane, acetone, isopropyl alcohol and distilled water, followed by drying with air blowing. The copper foil was heated with a rate of 20 $^\circ\text{C}/\text{min}$ up to 500 $^\circ\text{C}$ and held for 5 h under air atmosphere. After cooling down to room temperature, a dense array of copper oxide NWs was obtained on copper foil. The image of the copper oxide NWs was observed by scanning electron microscopy (SEM) and the crystal structure of nanowires was analyzed with X-ray diffraction analysis (XRD), transmission electron microscopy (TEM) and energy-dispersive X-ray spectroscopy (EDX) as shown in Figures 1(a), 2(a), 3 and 4.

Hydrothermal synthesis of cobalt oxide nanoparticles

A two-step synthesis method was used to produce cobalt oxide (Co_3O_4) nanoparticles (NPs), with the first step of precipitation into cobalt hydroxide and the second step of hydrothermal synthesis to make cobalt oxide NPs. The precursor cobalt chloride ($\text{CoCl}_2 \cdot 6\text{H}_2\text{O}$) was purchased (Alfa Aesar) and dissolved in distilled water in concentration of 1.0 M. To induce a precipitation of $\text{Co}(\text{OH})_2$, 10.0 M NaOH aqueous solution was added gradually until the pH of the mixed solution reached 11.5. The mixed solution was placed inside a Teflon liner of high pressure steel container and subjected to a hydrothermal synthesis for 20 h at 150 $^\circ\text{C}$.

After the synthesis, the remaining precursor solution and reaction byproducts were removed with repeated washing in distilled water followed by centrifuging, after which freeze-drying for 1 day was employed to dry the cobalt oxide nanoparticles. The dried particles were annealed at 750 $^\circ\text{C}$ for 2 h to fully crystallize into Co_3O_4 NPs. The processed Co_3O_4 NPs were composed of mainly particles having 100–200 nm in average size. The structure of the Co_3O_4 NPs was analyzed by SEM microscopy and XRD as shown in Figures 1(b) and 2(b).

Designs of SSC layers to increase optical absorption

Based on the evaluation of optical reflectance of CuO NWs alone and that of Co_3O_4 NPs alone (see Figure 6(a)), it is seen that copper oxide nanowires (NWs) can absorb a large amount of visible spectrum. By contrast, the coated layer of Co_3O_4 nanoparticles (NPs) exhibits a much higher optical reflectance in the visible range than CuO NWs, but shows an advantage of absorbing more near-IR spectrum than the CuO NWs. Therefore, a combined tandem structure of copper oxide NWs and cobalt oxide NPs was devised to take advantage of both materials unique characteristics and achieve higher absorption of sunlight in both near-IR and visible spectrum. The SEM micrograph of Figure 6(b) shows one example of such a combined tandem structure of CuO NWs and Co_3O_4 NPs. This concept of tandem structure formation for optically improved SSC layer is more clearly illustrated by schematic diagrams of Figure 5.

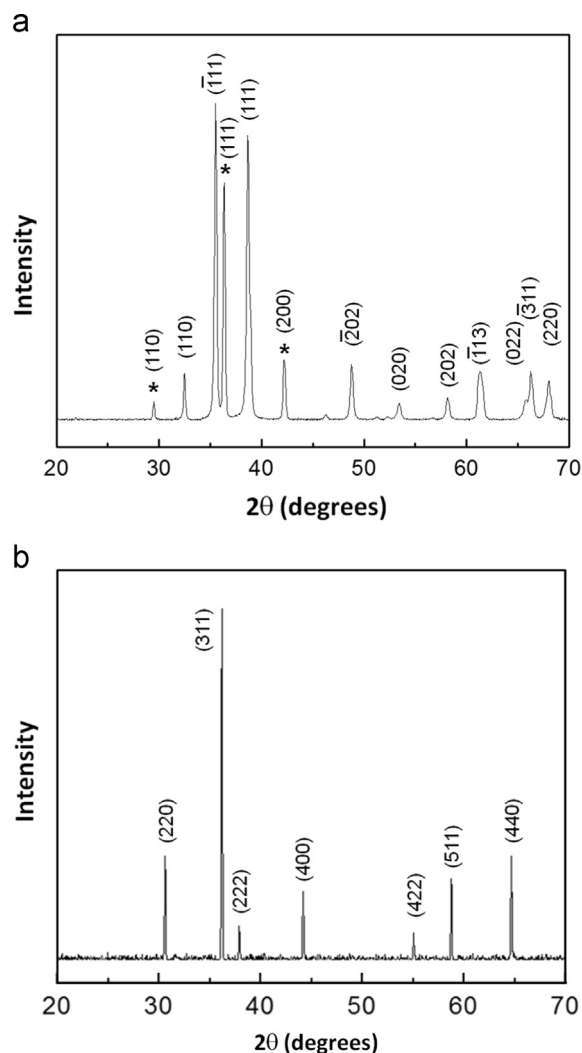


Figure 2 (a) XRD analysis of copper oxide nanowires (NWs) scraped off from the copper foil, showing two types of copper oxide consisting of CuO and Cu_2O phase (* mark) and (b) XRD analysis of cobalt oxide nanoparticles (NPs) exhibiting the crystal structure of Co_3O_4 .

According to Figure 5, vertically aligned CuO NWs and spherical Co_3O_4 NPs can be combined in two different configurations. One way is to coat the vertical CuO NWs with cobalt oxide NPs by means of spray-coating, or dip-coating method which makes micro-cone type of structure formed with cobalt oxide NPs, as shown in the left side procedure of Figure 5. Another way of tandem structure formation is to have the copper oxide NW layer itself separated from the copper foil substrate by wet-etching removal of Cu, followed by attachment of it on top of micro-layer of cobalt oxide NPs pre-deposited on Inconel substrate surface, as represented by the right side procedure of Figure 5.

Fabrication of tandem SSC layers

Spectrally selective coating (SSC) layer of copper oxide nanowires (NWs) combined with cobalt oxide (Co_3O_4) nanoparticles

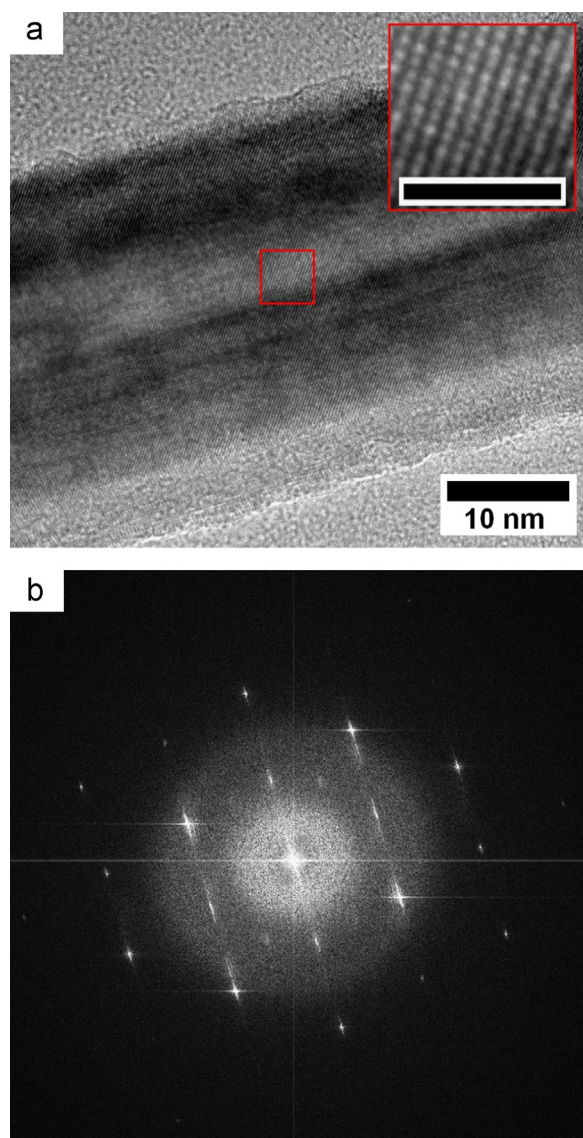


Figure 3 (a) Images of a single CuO nanowire by TEM analysis where an inset image is a magnified crystal structure of CuO for a red-lined square area (a black scale bar=2 nm) and (b) FFT patterns obtained from all area of the nanowire in Figure 3(a).

(NPs), was fabricated with three different methods including spray-coating, dip-coating, and transferring.

For the preparation of coating solution for spray-coating of the synthesized cobalt oxide NPs, phenyl-methyl polysiloxane resin (purchased from Evonik (Germany, SILIKOPHEN P 80/X)) was utilized as a binder resin. After diluting to 6 wt% by adding a cosolvent of isobutanol/xylene (1/3 v/v ratio) to the purchased resin solution, cobalt oxide NPs were then added to the diluted binder solution with a composition of 4:1 (w/w) (cobalt oxide: phenyl-methyl polysiloxane). In the final coating solution, the concentration of total solid consisting of cobalt oxide and a binder became 18 wt%. The nanoparticle dispersion was further improved by sonication followed by ball-mixing for 1 day. On the surface of copper oxide NWs (which are semi-vertically aligned on Cu foil surface), the final cobalt oxide NPs coating solution was spray-coated (left side schematics in Figure 5) after which the binder resin was cured at 250 °C for 1 h in air atmosphere.

Cobalt oxide solutions with different concentrations of 18 wt% and 6 wt% were used for the dip-coating of cobalt oxide NPs into the copper oxide NW structure. The cobalt oxide solution of 18 wt% prepared as described above was used for dip-coating into copper oxide NW structure with different dipping methods, including a continuous longer time dipping (10 min) without making the solution container to be vacuum state, and a dipping with 1 cycle of vacuum (20 s) and venting. For a diluted coating solution with a solid concentration of 6 wt%, the previous 18 wt% solution was diluted by a factor of 3 by adding isobutanol/xylene (1/3 v/v). With this diluted cobalt oxide solution (6 wt%), copper oxide NW structure was dip-coated using 1 cycle of vacuum/venting and 3 cycles of vacuum/venting procedure. For all these dip-coating procedures, the drying and curing procedure was carried out at 250 °C for 1 h in air environment.

For an alternative tandem structure by transferring of copper oxide NW layer and placing it on top of cobalt oxide NP layer (right side schematics in Figure 5), the copper oxide NWs grown thermally on copper foil were separated from the copper foil by wet-etching removal of remaining Cu in a mixed aqueous solution of 3.0 M iron chloride solution and 37% hydrochloric acid solution (25/1 w/w). Before transferring, thin binder resin layer of phenyl-methyl polysiloxane was coated on cobalt oxide NP layer (30 μm) formed on Inconel alloy (Type 625) substrate by spray-coating at 40 psi pressure, using the cobalt oxide NP solution with 18 wt% concentration. The separated copper oxide NW layer was transferred onto the binder resin layer, followed by drying and curing at 250 °C for 1 h in air atmosphere.

Optical reflectance measurement and figure of merit (FOM) evaluation

Visible/infrared (IR) reflectance of different types of SSC layers was measured, using a home-made reflectance measurement system consisting of an integration sphere (4" LabSphere[®], Spectrafect[®] coated) assembled with an Andor[®] Shamrock 303i spectrometer equipped with Si and InGaAs-based detectors. The optical reflectance was measured with

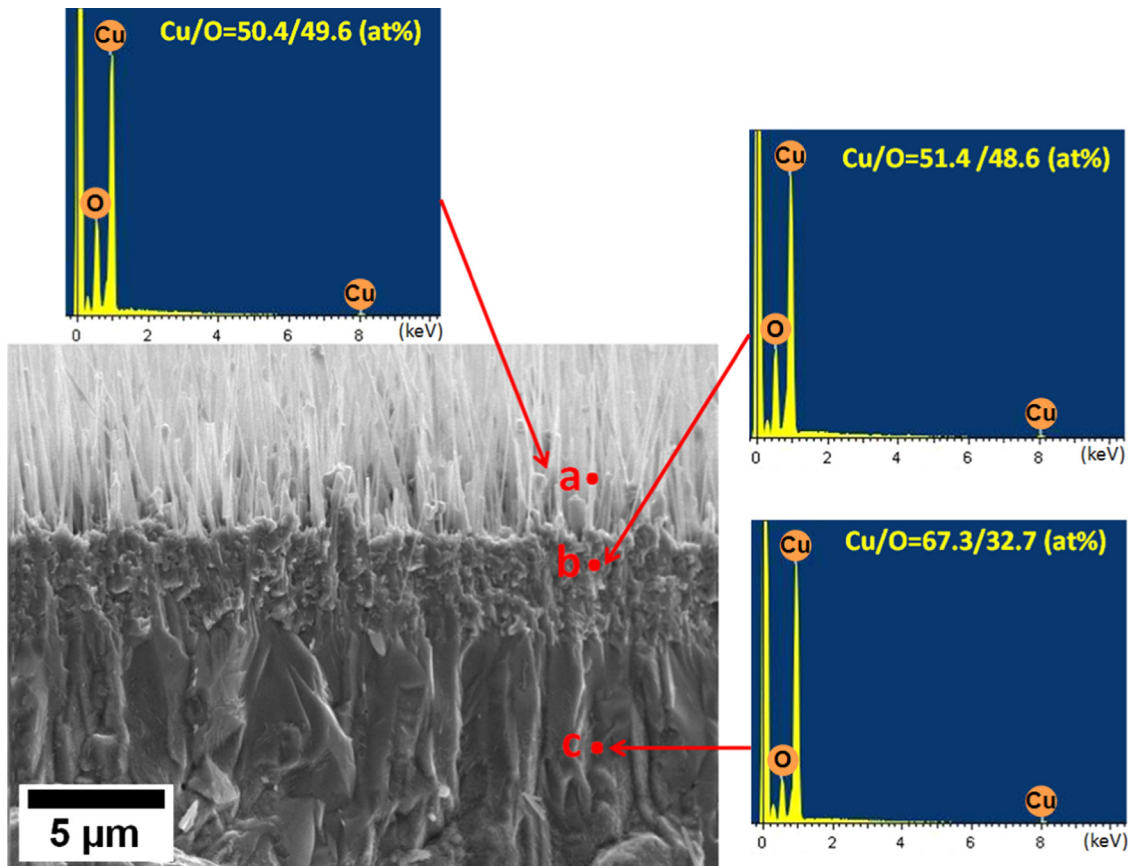


Figure 4 EDX analysis made with observation of a cross-sectional SEM image (tilt angle: 90°) of as-prepared copper oxide NWs layer showing two phases (CuO , and Cu_2O) depending on the position (a: nanowire at $2\ \mu\text{m}$ above nanowire bottom surface, b: $1.5\ \mu\text{m}$ underneath the nanowire bottom surface, and c: $8\ \mu\text{m}$ underneath the nanowire bottom surface). The small peaks at $0.2\text{--}0.4\ \text{keV}$ come from the carbon tape used for sample holding.

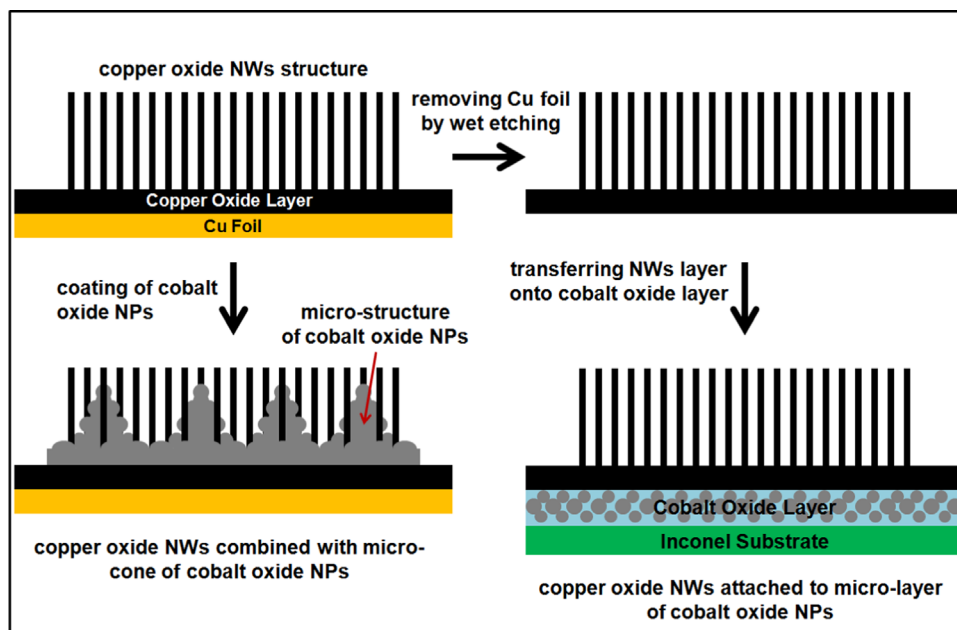


Figure 5 Schematic illustration of the tandem-structured spectrally selective coating (SSC) layer concepts including coating cobalt oxide NPs into vertically aligned copper oxide NWs as well as transferring of copper oxide NW layer onto the layer of cobalt oxide NPs.

incidence angle of 12.5° in the spectrum range of 400–2000 nm for SSC layers at room temperature.

To compare the absorption efficiency of the SSC layers for solar receivers, figure of merit (FOM) value was evaluated for various SSC layers including the tandem structured SSC layers. The figure of merit (FOM) is defined as follows (Eq. (1)).

$$F = \frac{\int_0^\infty (1-R(\lambda))I(\lambda)d\lambda - (1/C) \left[\int_0^\infty (1-R(\lambda))B(\lambda, T)d\lambda \right]}{\int_0^\infty I(\lambda)d\lambda} \quad (1)$$

where $R(\lambda)$ is the spectral reflectivity, $I(\lambda)$ is the spectral solar irradiance per square meter as defined by the reference solar spectral irradiation (ASTM G173), $B(\lambda, T)$ is the spectral thermal emission of a black body at temperature T , and C is the concentration ratio. For large concentration ratio of mirror-focused sunlight such as solar power tower type CSP generator systems, the optical absorption (related to optical reflectance properties) is the dominant factor.

XRD, TEM, EDX and SEM analysis

X-ray diffraction (XRD) analysis was carried out to investigate the crystal structure of copper oxide nanowires (NWs) and cobalt oxide nanoparticles (NPs). Copper oxide NWs were separated from copper foil by scraping off with a razor blade. Crystal structures of copper oxide NWs and cobalt oxide NPs were characterized by Bruker D2 Phaser XRD with $\text{Cu K}\alpha$ ($\lambda=0.154$ nm) as the radiation source. The scanning of 2θ angle (degree) was made in the range of 20 – 70° with a scanning rate of $1.0^\circ/\text{min}$.

In order to analyze more precisely the crystal structure of copper oxide nanowires, a single copper oxide nanowire was analyzed with transmission electron microscope (TEM) (FEI Tecnai F20 G²) operated at the acceleration voltage of 200 kV in bright field (BF) mode and high resolution (HR) mode, followed by fast Fourier transform (FFT) analysis to confirm the crystal structure of the nanowire.

The copper oxide phases existing at different positions in the cross-sectional area of copper oxide NW structure were analyzed using energy-dispersive X-ray spectroscopy (EDX) installed with scanning electron microscopy (SEM) (Oxford), with an acceleration voltage of 10 kV. The structures of copper oxide NWs, cobalt oxide NPs, and the combined tandem structured SSC layers were imaged by SEM.

Results and discussion

Characterization of copper oxide NWs and cobalt oxide NPs

The XRD analysis indicates that the scraped-off copper oxide nanowires (NWs) have two crystal phases including CuO phase and Cu_2O phase (* mark) as shown in Figure 2(a). For CuO crystal structure, two main planes of $(\bar{1}11)$ and (111) are observed at $2\theta=35.6^\circ$ and 38.7° , respectively in end-centered monoclinic system [28]. For Cu_2O crystal structure there are three planes including (110) , (111) and (200) at $2\theta=29.5^\circ$, 36.3° , and 42.3° , respectively in the primitive cubic system [29]. CuO phase can come from the crystal structure of nanowires and Cu_2O phase in XRD

analysis can originate from the material in the copper oxide bottom layer from which the copper oxide NWs grow. Because the some chunks of bottom layer can be taken out together with nanowires during the strong scraping during the razor blade removal process.

In addition to the previous research on CuO NWs [13], our TEM and EDX analyses also confirm that the copper oxide nanowire is composed of only CuO crystal phase with band gap of 1.2–1.4 eV while the bottom layer copper oxide (from which the CuO nanowires grow) contains CuO in the upper portion of the layer while some Cu_2O phase is present in the lower part of the bottom oxide layer. The Cu_2O phase is known to be a larger band gap copper oxide with 2.17 eV [18,19]. The crystal structure of a single copper oxide nanowire is shown in the inset of the TEM image in Figure 3(a). The FFT pattern in Figure 3(b) obtained for all area of the nanowire in Figure 3(a) shows that the copper oxide nanowire consists of only CuO phase containing (101) , (110) , (111) , $(\bar{2}02)$, (202) , (022) and $(\bar{2}04)$ plane which corresponds to lattice plane spacing of 3.138 Å, 2.739 Å, 2.356 Å, 1.885 Å, 1.570 Å, 1.425 Å and 1.195 Å, respectively. The cross-sectional SEM image of CuO NW layer obtained by tilting 90° was analyzed by EDX analysis at three points (a: nanowire at $2\ \mu\text{m}$ above the nanowire bottom surface, b: $1.5\ \mu\text{m}$ underneath the nanowire bottom surface (within the bottom copper oxide layer), and c: $8\ \mu\text{m}$ underneath the nanowire bottom surface) as exhibited in Figure 4. This EDX analysis at point a on nanowires indicates that the composition of overall nanowires is $\sim 1/1$ (Cu/O) in atomic ratio which is in accordance with CuO phase as identified by TEM and FFT in Figure 3. The first point beneath nanowire's bottom surface (point b) is confirmed to be composed of $\sim 1/1$ (Cu/O) in atomic ratio corresponding to CuO phase, while the second point beneath the nanowire bottom surface (point c) shows $\sim 2/1$ (Cu/O) in atomic ratio matching with Cu_2O phase.

The nanowire layer (above 5 μm thickness) is all made of CuO phase as identified by TEM. The upper portion of the oxide layer (from which the CuO nanowires grow) is $\sim 5\ \mu\text{m}$ thick and also CuO phase as identified by EDX analysis. The lower portion of the bottom oxide layer contains some Cu_2O . Therefore, the optical reflectance behavior is mostly dominated by the CuO phase which is located at outermost two layers having total thickness of above 10 μm . During CSP operation at high temperature, it is likely that the Cu_2O phase will eventually oxidize further to become CuO, which is considered to be a beneficial reaction. For study of the stability of CuO phase at high temperature, the copper oxide nanowire layer was annealed at 500°C for 10 h under air atmosphere and the overall atomic composition of Cu/O was measured with EDX as shown in Figure S1. The atomic composition of CuO in nanowires and in the upper portion of the oxide bottom layer are stable enough to maintain $\sim 1/1$ ratio of Cu/O, which implies that the formed CuO phase can be expected to retain the stable crystal structure and optical properties during CSP operation.

Figure 2(b) shows XRD analysis of cobalt oxide nanoparticles (NPs) annealed at 750°C for 2 h in air. This analysis confirms that the hydrothermally synthesized cobalt oxide NPs are Co_3O_4 phase which has a main plane of (311) at $2\theta=36.2^\circ$ in face-centered cubic system [30].

The SEM image in Figure 1(a) shows that the copper oxide NWs are longer than 5 μm in length and have 100–200 nm in diameter as can be seen more clearly in an inset image in

Figure 1(a). The spacing between adjacent nanowires appears to be roughly 500 nm-2 μ m. The aspect ratio of nanowires is higher than ~ 25 , which is believed to be beneficial for higher absorption efficiency due to light trapping effect [9-12]. The SEM image in Figure 1 (b) exhibits that cobalt oxide NPs annealed at 750 $^{\circ}$ C for 2 h have mainly 100-200 nm in particle size, although some particles have a diameter as small as 50 nm.

Tandem structured SSC layer by spray-coating

Tandem structure of solar absorbers can be fabricated with copper oxide nanowires (NWs) coated with the solution of cobalt oxide nanoparticles (NPs) by means of either spray-coating or dip-coating with the aforementioned concept explained in the left side procedure of Figure 5.

Spray-coating of cobalt oxide NPs solution is made onto copper oxide NW layer of Figure 1(a). Due to the vertically aligned nanowire structure of copper oxide, the cobalt oxide solution, even with nanoparticle size, is difficult to uniformly penetrate all the way down to the bottom of nanowires through their interspace gap regions. Therefore, a micro-ball type of cobalt oxide structure with a partial

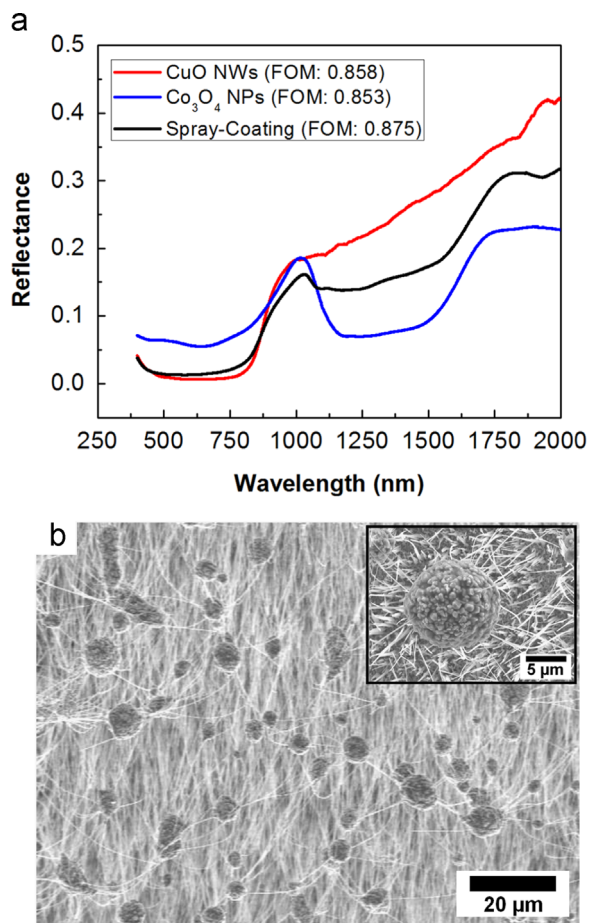


Figure 6 (a) Comparison of the optical reflectance and FOM between the tandem SSC layer by spray-coating, and the SSC layer of copper oxide NWs only, or the SSC layer of cobalt oxide NPs only and (b) SEM image of tandem SSC layer made by spray-coating of cobalt oxide NPs onto vertical copper oxide NWs.

penetration into copper oxide NWs is formed when spray-coating is carried out, as shown in Figure 6(b). Even though the cobalt oxide NPs are not infiltrated into the bottom of the CuO nanowire array, the optical reflectance data in Figure 6(a) shows that this type of tandem structure decreases near-IR reflectance due to the absorption of near-IR by Co_3O_4 NPs. The reflectance of visible light spectrum increases slightly compared to the copper oxide NWs only structure due to the addition of some Co_3O_4 NPs. The figure of merit (FOM) value increases a little from 0.858 to 0.875 when the copper oxide NWs is hybridized into a tandem structure with the addition of cobalt oxide NPs by spray-coating because the overall absorbed solar energy is larger in cobalt oxide NPs-sprayed copper oxide NWs due to the more substantial reduction of reflectance in the near-IR spectrum range relatively to the increment of the reflectance in the visible spectrum range.

Tandem structured SSC layer by dip-coating

Comparison of optical reflectance and FOM among different SSC layers, shown in Figure 7(a), indicates that the optical reflectance properties are sensitive to the SSC layer structures and how they are produced. As compared to the rapid spray-coated structures, a slower process of dip-coating allows the cobalt oxide nanoparticles (NPs) to penetrate deeper into the spaces between copper oxide nanowires (NWs) having a relatively small spacing of ~ 500 nm to 2 μ m between adjacent nanowires. In addition, cobalt oxide NPs can also be entangled with copper oxide NWs, which may enable the formation of multi-scaled structures composed of the combination of microscale and nanoscale structures of nanowires and nanoparticles, as observed in Figure 7(c-1-d-2). The presence of some pore structures may also contribute to enhanced sunlight absorption. In order to make cobalt oxide NPs to infiltrate into copper oxide NW structures more efficiently, a cycle of vacuum suction/venting process is devised for the dip-coating process. The vacuum is not a high vacuum but a typical, mechanical pump type of low vacuum was sufficient. The vacuum process extracts and removes most of entrapped air from copper oxide NWs structure, and this process causes the cobalt oxide NPs in solution to be sucked into the spaces that the air pocket previously occupied. Subsequent venting step allows the air to come in which generates such a large pressure difference between vacuum state and atmospheric pressure that cobalt oxide NP solution is pushed and driven into the interspace of aligned copper oxide NWs. Repeated vacuum/vent processes further controls the formation of tandem mixed structure and the sunlight absorption and the FOM properties are accordingly also affected as will be discussed later.

It is seen that without using the vacuum/venting process, the cobalt oxide NPs hardly get into the inter-nanowire spacing, as can be seen in Figure 7(b) but instead cover up the surface of the CuO nanowire structure as an almost continuous particle layer. Copper oxide NWs are rarely seen to protrude out of the cobalt oxide NP layer, except a few NWs which has very little affect on optical properties of SSC layers. As expected, the optical reflectance data of this monotonous structure shows a similar reflectance behavior

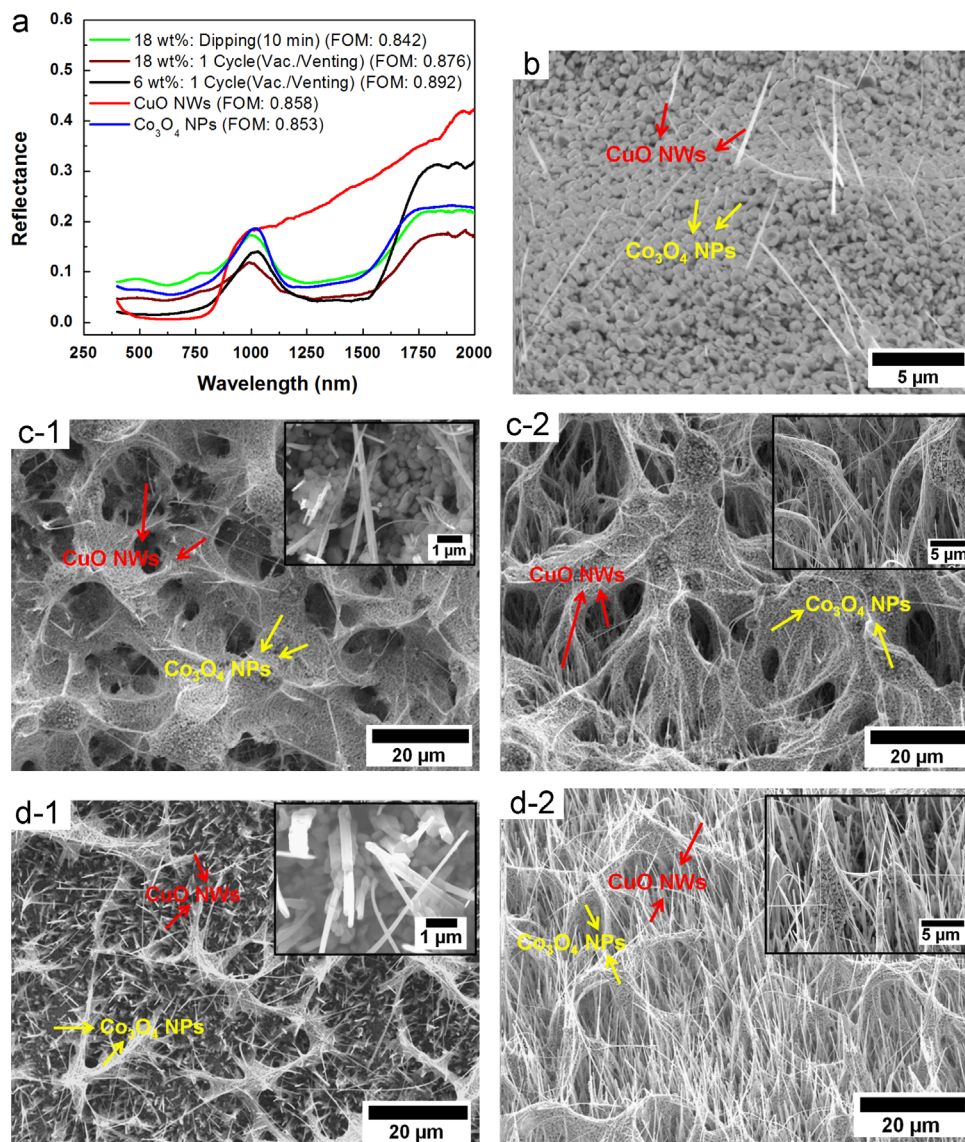


Figure 7 (a) Comparison of optical reflectance and FOM among different SSC layers, (b) a top view surface image of tandem SSC layer made by 10 min dip-coating in 18 wt% cobalt oxide solution without using a vacuum process, (c-1) a top view surface image and (c-2) a tilted surface image of tandem SSC layer made by dip-coating with 1 cycle of vac./venting in 18 wt% cobalt oxide solution, and (d-1) a top view surface image and (d-2) a tilted surface image of tandem SSC layer made by dip-coating with 1 cycle of vac./venting in 6 wt% cobalt oxide solution.

to that of the SSC layer fabricated with cobalt oxide NPs only (Figure 7(a)) and the FOM value of this structure is only 0.842 which is not high enough to absorb sufficient solar energy. This dip-coated sample without using vac./venting procedure produces a structure covered mostly with Co₃O₄ particles, with very few number of CuO nanowires protruding (Figure 7(b)), so it is essentially Co₃O₄ particle surface. The spray-coating method to produce the Co₃O₄ particle SSC layer tends to have a high porosity and roughness as represented in Figure S2. Therefore, the Co₃O₄ layer of Figure S2 produces a slightly lower reflectance in the visible spectrum range.

The vacuum/venting process was utilized to make further advanced dip-coating structures with the concentrated solution of 18 wt%. After placing the copper oxide NW sample into cobalt oxide NP solution, the vacuum is made for 20 s followed by a

fast venting process with air, which may cause some interesting mechanical disturbance on the coating structure. As shown in Figure 7(c-1) and (c-2), copper oxide NWs and cobalt oxide NPs form combined complex structures where copper oxide NWs are entangled with themselves coated with cobalt oxide NPs. In more details, a top side of this sample displays a spire-like roof layer of cobalt oxide NPs in Figure 7(c-1) whose inset image shows the bottom surface coated with cobalt oxide NPs at interspaces between the copper oxide NWs. The tilted images including a magnified inset image in Figure 7(c-2) exhibit the entangled tripod-like structure of copper oxide NWs mixed with cobalt oxide NPs. Figure 7(a) demonstrates that this 3-dimensionally entangled tripod-like structure can decrease the reflectance in both visible and near-IR spectrum regime and obtain a higher FOM value of 0.876, compared to the sample made by a continuous dipping (Figure 7(b)).

To better control the degree of entangling of copper oxide NWs and agglomeration of cobalt oxide NPs, the dip-coating solution was diluted to 6 wt%, that is, 1/3 of initial concentration, as the third approach. This third dip-coating method also uses the procedure of vacuum/venting, but due to the reduced solid concentration of nanoparticles and the binder resin, the insertion of the nanoparticles into the nanowire spacing gets easier. From the top view surface image (Figure 7(d-1)) and a tilted view (Figure 7(d-2)), the occupied area by a spire-like top layer of cobalt oxide NPs is diminished (Figure 7(d-1)) and micro-cone structure of cobalt oxide NPs is formed (see the inset of Figure 7(d-2)) instead of the tripod-like structure observed in Figure 7(c-2). The dip-coating with a diluted solution of 6 wt% essentially maintains the nanowire structure of copper oxide after the dip-coating of cobalt oxide NPs so that a more or less uniform multi-scaled micro-nano structure can be made, which can be more effective in absorbing sunlight in both visible spectrum and near-IR spectrum.

Optical reflectance measurements in Figure 7(a) shows that this multi-scaled tandem structure (Figure 7(d-1) and (d-2)) coated with the diluted solution of 6 wt% exhibits much lower reflectance in visible spectrum and similarly reduced reflectance in near-IR spectrum range, compared to the entangled tripod-like structure (Figure 7(c-1) and (c-2)) made of cobalt oxide solution with higher concentration of 18 wt%. The FOM value of this structure increases up to 0.892 which is much higher than the structure of Figure 7(c-1) and (c-2). The lower reflectance in visible spectrum results from the well-preserved nanowire structure of copper oxide and the similarly low reflectance of near-IR (1.0-1.55 μm) is attributed to the cone-type of microstructure of cobalt oxide NPs as well as the layer of cobalt oxide NPs coated on the bottom of copper oxide NWs as can be seen in the inset of Figure 7(d-1). In the spectrum ranging from 1.55 μm to 2.0 μm , the dip-coated layer with 6 wt% solution shows a steeper increase of reflectance than that with 18 wt% solution. The diluted 6 wt% Co_3O_4 particles layer has less amount of Co_3O_4 than the 18 wt% Co_3O_4 layer. It can be recognized that Co_3O_4 particles layer reflects less IR spectrum ranging from 1.0 μm to 2.0 μm than CuO nanowires layer as can be compared in Figure 7(a). Lower concentration of Co_3O_4 particles can make thinner layer of Co_3O_4 particles and will result in less absorption which enable the SSC layer to have higher reflectance in IR spectrum compared to SSC layer coated with an 18 wt% solution (brown-colored graph in Figure 7(a)). This behavior of reflectance increasing steeply from 1.55 μm will be useful for the CSP or other solar thermal application which needs to have cut-off wavelength around 1.55 μm in order to reduce the emission loss of infrared spectrum. For instance, in the parabolic trough type concentrated solar power systems, the cut-off wavelength of 1.5 μm is helpful to increase FOM value by diminishing the amount of IR emission at 700 $^\circ\text{C}$ [4].

To optimize the procedure of vacuum/venting cycle, the dip-coating is also made with 3 cycles of vacuum/venting by which more cobalt oxide NP material is pushed into the CuO NW structure so that an increased amount of cobalt oxide layer is expected to be deposited onto the bottom of CuO NW structure. The inset image of Figure 8(a) shows that the bottom of copper oxide NWs is covered with cobalt oxide NPs. Repeated vacuum/vent processes further controls the formation of

tandem mixed structure with more cobalt oxide NPs deposited, with the sunlight absorption and the FOM properties accordingly affected. For example, 3 cycles of vacuum/venting process for dip-coating with the diluted solution of 6 wt% forms a somewhat larger area of a spire-like roof layer of cobalt oxide NPs

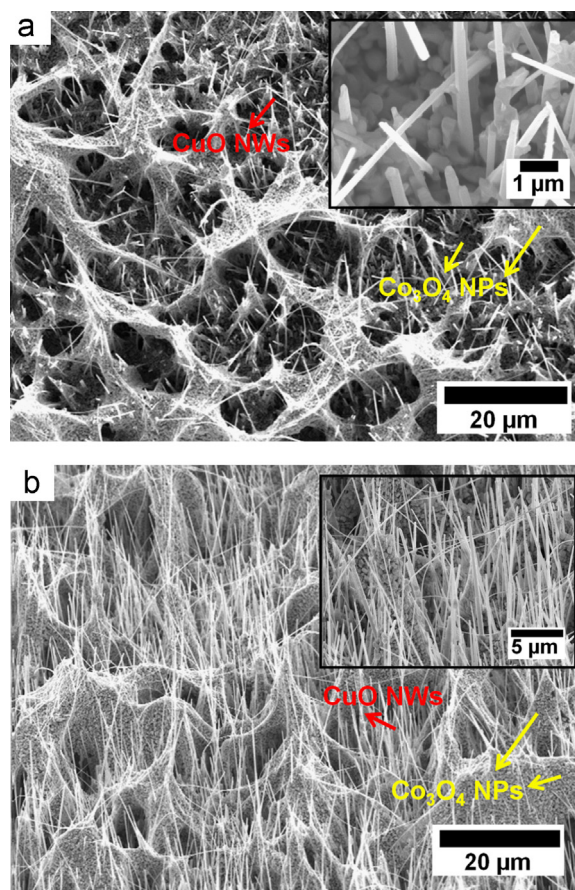


Figure 8 SEM images showing (a) a top view surface image and (b) a tilted surface of tandem SSC layer made by dip-coating with 3 cycles of vac./venting procedures in 6 wt% cobalt oxide solution.

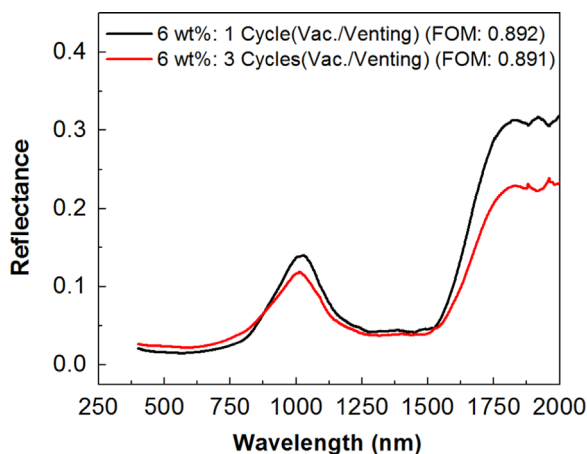


Figure 9 Optical reflectance measured and FOM values calculated for tandem SSC layer fabricated by dip-coating with 1 cycle of vac./venting process and 3 cycles of vac./venting process in 6 wt% cobalt oxide solution.

(Figure 8(a)), compared to the structure made with just 1 cycle of vacuum/venting procedure (Figure 7(d-1)). From tilted images in Figure 8(b), it can be observed that cobalt oxide NPs form micro-cone structure similar to the structure in the inset image of Figure 7(d-2).

Optical reflectance measurement in Figure 9 indicates that the 3 cycle procedure slightly increases the reflectance of visible spectrum but noticeably decreases the reflectance of near-IR as well as short wavelength IR (SWIR) spectrum. The small increase of reflectance in the visible spectrum results from the diminished nanowire structure of copper oxide caused by the addition of more nanoparticles and wider spire-like roof area of cobalt oxide NPs. The thicker cobalt oxide layer which can be expected by 3 repetition cycles absorbs a larger amount of sunlight SWIR spectrum (1.6–2.0 μm) to result in the decreased reflectance in that wavelength regime. In the IR spectrum range, the spectrum of 0.8–1.6 μm is more important to a solar absorber due to its higher energy than longer IR spectrum above 1.6 μm . So the SSC layer made by 3 cycles of vacuum/vent processing has FOM value of 0.891 which is very similar to that (0.892) of SSC layer by 1 cycle dip-coating.

For a contrast experiment, a SSC layer was fabricated using the mixture solution (1/1 w/w) of Co_3O_4 particles and CuO nanowires which were scraped off from the copper foil. Using the same condition and ball-mixing procedure as the previous Co_3O_4 layer, the mixture solution was spray-coated on Inconel substrate and the reflectance of the sample was measured. Figure S3 indicates that the reflectance of the mixture sample is much higher in all spectrum range than the dip-coated SSC layer made with 6 wt% and vac./venting procedure. One possible reason for such a behavior is that the nanowires can be inadvertently shortened much during the ball-mixing process, thus the SSC layer has no structure advantage on entrapping sunlight, compared to SSC layer of vertically standing nanowires.

Tandem structured SSC layer by transferring of copper oxide NW layer

Copper oxide nanowire (NW) layer separated from Cu foil is composed of a horizontally configured copper oxide flat layer (1–2 μm thick) at the bottom from which copper oxide NWs have grown, as indicated in Figure 10(a). Figure 10(b) represents the final attached structure consisting of copper oxide NWs layer / polysiloxane binder resin layer / cobalt oxide NPs layer. It is expected that pure copper oxide NWs layer without cobalt oxide NPs is able to absorb more visible spectrum while the cobalt oxide NPs layer under copper oxide NW layer can absorb the near-IR spectrum transmitted through the copper oxide NW layer positioned above the nanoparticle layer, as explained in the aforementioned concept section (Figure 5).

The reflectance of visible spectrum is similarly as low as the pure copper oxide NW sample, but the reflectance of near-IR spectrum is not decreased as low as pure cobalt oxide layers, as shown in Figure 11. The data in Figure 11 indicates that the reflectance value in the near-IR spectrum for the SSC layer fabricated by transferring the CuO NW layer is higher than that for the SSC layer of pure cobalt oxide NPs and lower than that for the SSC layer of pure copper oxide NWs, as well as SSC

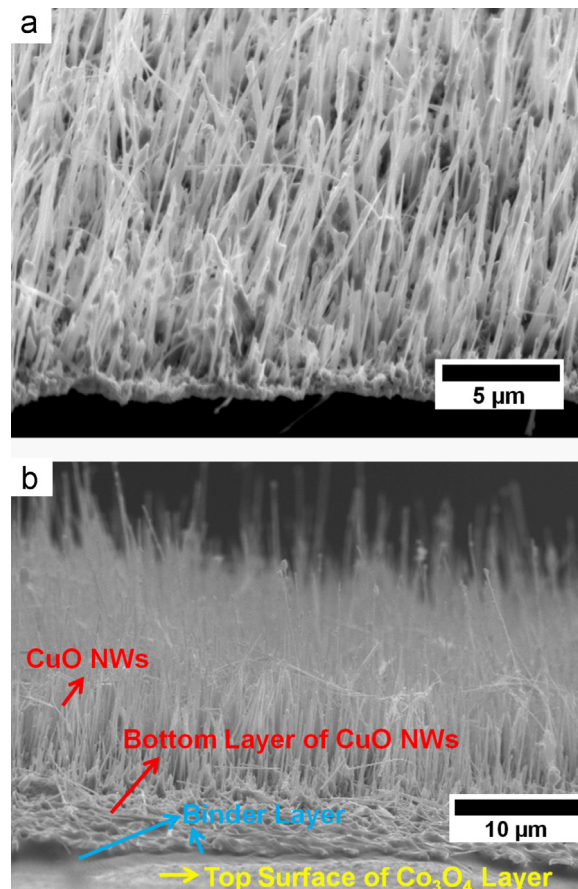


Figure 10 SEM images representing (a) a stand-alone copper oxide NWs layer obtained by etching Cu metal layer, and (b) a transferred copper oxide NWs layer attached onto cobalt oxide layer with a thin binder resin layer.

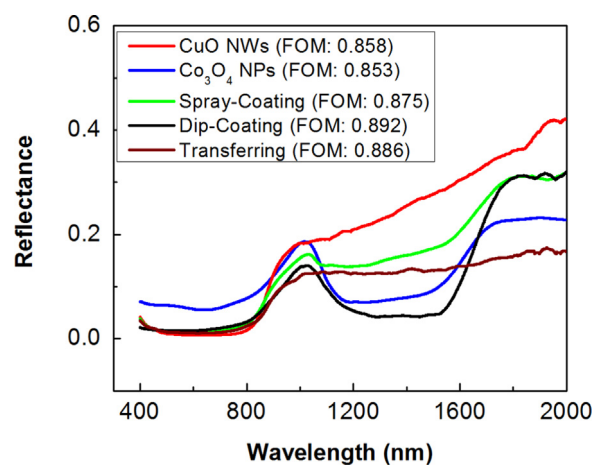


Figure 11 Optical reflectance and FOM compared among structured SSC layers including a copper oxide NWs layer only, a cobalt oxide NPs layer only, a spray-coated tandem SSC layer, a dip-coated tandem SSC with 1 cycle of vac./venting process in 6 wt% cobalt solution, and a transferred tandem SSC layer.

layer made by the spray-coating. Copper oxide NWs may reflect near-IR spectrum partially before it is transmitted to the bottom layer of Co_3O_4 NPs. Table 1 shows FOM values of the representative SSC layers including SSC layer fabricated by

Table 1 Calculated FOM values from reflectance measurement of SSC layers.

SSC layers	FOM
Copper oxide NWs only	0.858
Co ₃ O ₄ NPs only	0.853
Tandem SSC by spray-coating	0.875
Tandem SSC by dip-coating (1 cycle, 6 wt%)	0.892
Tandem SSC by transferring	0.886

the transfer method. The tandem SSC layer by transferring has FOM value of 0.886 which is much higher than that of pure copper oxide NWs, pure cobalt oxide NPs and spray-coated SSC layers, but lower than that of efficiently dip-coated SSC layer.

Conclusion

Tandem-structured spectrally selective coating (SSC) layer was newly devised with novel and scalable methods to increase the absorption efficiency of solar spectrum. This new SSC layer structure is simultaneously utilizing the thermally grown copper oxide NWs and the hydrothermally synthesized cobalt oxide NPs. The tandem-structured SSC layer consists of a multi-scaled combination of copper oxide nanowire (NW) layer having a good visible light absorbing material and structure, together with wet-coated microstructure of cobalt oxide nanoparticles (NPs) having a good near-IR absorbing characteristics. Various novel structured SSC layers were built with 3 different fabrication methods including the spray-coating, vacuum/vent processed advanced dip-coating of cobalt oxide NPs into copper oxide NWs forest, and the transferring of copper oxide NWs layer onto cobalt oxide layer. The tandem-structured SSC layers exhibited superior light absorbing properties in the visible and near-IR spectrum range, with much higher figure of merit (FOM) values close to ~0.90. These tandem structures and fabrication procedures to achieve higher and wider absorption of solar spectrum can be highly useful for enhanced solar absorption in the field of solar energy conversion systems such as concentrated solar thermoelectric generators and concentrating solar power systems.

Acknowledgment

The support of this research by Department of Energy through DOE SunShot Project (DE-EE0005802) is acknowledged.

Appendix A. Supporting information

Supplementary data associated with this article can be found in the online version at <http://dx.doi.org/10.1016/j.nanoen.2014.10.018>.

References

- [1] G. Brumfiel, *Nature* 436 (2005) 318-320.
- [2] J. Beer, W. Mende, R. Stellmacher, *Quat. Sci. Rev.* 19 (2000) 403-415.
- [3] D.E. Carlson, C.R. Wronski, *Appl. Phys. Lett.* 28 (1976) 671-673.
- [4] J. Moon, D. Lu, B. VanSaders, T.K. Kim, S.D. Kong, S. Jin, R. Chen, Z. Liu, *Nano Energy* 8 (2014) 238-246.
- [5] D. Kraemer, B. Poudel, H.-P. Feng, J.C. Caylor, B. Yu, X. Yan, Y. Ma, X. Wang, D. Wang, A. Muto, K. McEnaney, M. Chiesa, Z. Ren, G. Chen, *Nat. Mater.* 10 (2011) 532-538.
- [6] L.L. Baranowski, G.J. Snyder, E.S. Toberer, *Energy Environ. Sci.* 5 (2012) 9055-9067.
- [7] A. Fujishima, K. Honda, *Nature* 238 (1972) 37-38.
- [8] M. Green, K. Emery, Y. Hishikawa, W. Warta, E. Dunlop, *Prog. Photovolt.: Res. Appl.* 20 (2012) 12-20.
- [9] K. Peng, Y. Xu, Y. Wu, Y. Yan, S.-T. Lee, J. Zhu, *Small* 1 (2005) 1062-1067.
- [10] L. Tsakalakos, J. Balch, J. Fronheiser, B.A. Korevaar, O. Sulima, J. Rand, *Appl. Phys. Lett.* 91 (2007) 233117-1-233117-3.
- [11] M.D. Kelzenberg, S.W. Boettcher, J.A. Petykiewicz, D.B. Turner-Evans, M.C. Putnam, E.L. Warren, J.M. Spurgeon, R. M. Briggs, N.S. Lewis, H.A. Atwater, *Nat. Mater.* 9 (2010) 239-244.
- [12] J. Zhu, Y. Cui, *Nat. Mater.* 9 (2010) 183-184.
- [13] X. Jiang, T. Herricks, Y. Xia, *Nano Lett.* 2 (2002) 1333-1338.
- [14] A. Kargar, Y. Jing, S.J. Kim, C.T. Riley, X. Pan, D. Wang, *ACS Nano* 7 (2013) 11112-11120.
- [15] W.H. Strehlow, E.L. Cook, *J. Phys. Chem. Ref. Data* 2 (1973) 163-199.
- [16] B.E. Deal, A.S. Grove, *J. Appl. Phys.* 36 (1965) 3770-3778.
- [17] T.K. Kim, J. Moon, B. VanSaders, D. Chun, C.J. Gardner, J.-Y. Jung, G. Wang, R. Chen, Z. Liu, Y. Qiao, S. Jin, *Nano Energy* 9 (2014) 32-40.
- [18] J. Ghijsen, L.H. Tjeng, J. van Elp, H. Eskes, J. Westerink, G.A. Sawatzky, *Phys. Rev. B* 38 (1988) 11322-11330.
- [19] F.P. Koffyberg, F.A. Benko, *J. Appl. Phys.* 53 (1982) 1173-1177.
- [20] J.G. Cook, M.P. Van Der Meer, *Thin Solid Films* 144 (1986) 165-176.
- [21] P. Nkeng, G. Poillerat, J.F. Koenig, P. Chartier, B. Lefez, J. Lopitaux, M. Lenglet, *J. Electrochem. Soc.* 142 (1995) 1777-1783.
- [22] P. Ruzakowski Athey, F.K. Urban III, M.F. Tabet, W.A. McGahan, *J. Vac. Sci. Technol. A* 14 (1996) 685-692.
- [23] C.-S. Cheng, M. Serizawa, H. Sakata, T. Hirayama, *Mater. Chem. Phys.* 53 (1998) 225-230.
- [24] D. Barreca, C. Massignan, S. Daolio, M. Fabrizio, C. Piccirillo, L. Armelao, E. Tondello, *Chem. Mater.* 13 (2001) 588-593.
- [25] H. Keppner, J. Meier, P. Torres, D. Fischer, A. Shah, *Appl. Phys. A* 69 (1999) 169-177.
- [26] G. Conibeer, M. Green, E.-C. Cho, D. König, Y.-H. Cho, T. Fangsuwannarak, G. Scardera, E. Pink, Y. Huang, T. Puzzer, S. Huang, D. Song, C. Flynn, S. Park, X. Hao, D. Mansfield, *Thin Solid Films* 516 (2008) 6748-6756.
- [27] K.A. Bertness, S.R. Kurtz, D.J. Friedman, A.E. Kibbler, C. Kramer, J.M. Olson, *Appl. Phys. Lett.* 65 (1994) 989-991.
- [28] S. Asbrink, A. Waskowska, *J. Phys.: Condens. Matter* 3 (1991) 8173-8180.
- [29] R. Restori, D. Schwarzenbach, *Acta Crystallogr. B* 42 (1986) 201-208.
- [30] J.P. Picard, G. Baud, J.P. Besse, R. Chevalier, *J. Less-Common Met.* 75 (1980) 99-104.



Tae Kyoung Kim is a Ph.D. candidate in the Materials Science and Engineering Program at University of California, San Diego (UCSD). He obtained B.S. and M.S. degrees from Yonsei University (South Korea) and had worked at Samsung Cheil Inc. (presently, Samsung SDI) as a senior researcher mainly in the field of materials for renewable energy generation and storage systems. And then he has been studying and researching in UCSD since 2011.



Bryan VanSaders is a Ph.D. graduate student in the Material Science and Engineering Program at University of California, San Diego (UCSD). He obtained his B.S. degree from Rutgers University and M.S. degree from UCSD. He has focused on nano-scale optics, plasmonics, and optical metamaterials.



Jaeyun Moon is an Assistant Professor of Mechanical Engineering at University of Nevada at Las Vegas (UNLV). She received her Ph.D. degree in the Materials Science and Engineering Program from University of California, San Diego (UCSD). She obtained her B.S. and M.S. degrees from Hanyang University (South Korea) and then had worked at Samsung Electronics as a senior engineer until 2009. Her research interest is renewable energy generations, especially the development and improvement of thermal energy conversion technologies such as concentrated solar power and thermoelectrics, using materials design and electrical/thermal characterization techniques.



Taewoo Kim is a graduate student in the Materials Science and Engineering Program at the University of California, San Diego (UCSD). He obtained B.S. degree in Chemistry Department from Korea Military Academy (South Korea) and had worked at Korea army as a company commander. And then he has been studying and researching in UCSD since 2013. His research interest is to develop nanoparticles and 3-dimensional porous structure.



Chin-Hung Liu is a Ph.D. candidate in the Materials Science and Engineering Program at University of California, San Diego (UCSD). He obtained B.S. degree from National Cheng Kung University (Taiwan, R.O.C.) and M.S. degree from National Tsing Hua University (Taiwan, R.O.C.). He mainly focuses on solar cells, In-As III-V semiconductors and Nd-Fe-B permanent magnets. He has been studying and researching at UCSD since 2011.



Jirapon Khamwannah received her B.S. degree (2006) in Materials Engineering from King Mongkut's University of Technology Thonburi, Thailand. She is currently Ph.D. candidate in Materials Science and Engineering Program at University of California, San Diego. Her research mainly focuses on advanced nanostructure materials and 3-D structure for applications in Dye-sensitized solar cells.



Dongwon Chun is a Ph.D. student in the Materials Science and Engineering Program at University of California, San Diego (UCSD) since 2012. He obtained B.S. and M.S. degrees from Yonsei University (South Korea) and had worked at the Korea Institute of Science and Technology as a research scientist mainly working on the Bio-MEMs and Materials Analysis.



Duyoung Choi is a Ph.D. candidate in the Materials Science and Engineering Program at the University of California, San Diego (UCSD). He obtained B.S. and M.S. degrees from Inha University (South Korea). He has been studying and researching on graphene and transition metal oxide composite for renewable energy generation and storage systems in UCSD since 2009.



Alireza Kargar is a Ph.D. candidate in the Electrical and Computer Engineering Department of the University of California, San Diego. He received B.S. degree from Shiraz University in Shiraz, Iran. His current research interests are design and fabrication of different nanostructures for solar energy conversion devices with focus on solar fuel generation systems.



Renkun Chen received his B.S. degree in Thermo-physics from Tsinghua University in 2004, and a Ph.D. degree in Mechanical Engineering from University of California, Berkeley in 2008. Following a one-year stint as a postdoctoral fellow at Lawrence Berkeley National Laboratory, he joined University of California, San Diego as an Assistant Professor in the Department of Mechanical and Aerospace Engineering in 2009. His research interests include nanoscale heat transfer, energy conversion materials, and thermal management.



Zhaowei Liu is an Assistant Professor of Electrical and Computer Engineering at University of California, San Diego (UCSD). He received his Ph.D. in mechanical engineering (MEMS/Nanotechnology) from University of California, Los Angeles in 2006. Before joining UCSD faculty, he was a post-doctoral researcher at the NSF Nanoscale Science & Engineering Center (NSEC) in the Mechanical Engineering Department at University of California, Berkeley. His research interest includes nanophotonics, plasmonics, metamaterials, energy and ultrafast opto-electronics.



Sungho Jin received his B.S degree in Metallurgical Engineering from Seoul National University in 1969, and Ph.D. degree in Materials Science & Engineering from University of California, Berkeley in 1974. After 26 years of R&D at Bell Laboratories at Murray Hill, New Jersey, he joined University of California, San Diego (UCSD) in 2002 as a Professor and Iwama Endowed Chair. He is currently a Distinguished Professor at UCSD, and is serving as the Direc-

tor of UCSD-wide Materials Science & Engineering Program. His research interests include R&D of nano materials, magnetic materials, electronic materials, energy materials, and bio materials.